Zitierweise: *Angew. Chem. Int. Ed.* **2024**, e202406440
doi.org/10.1002/anie.202406440

Frustrated Lewis Pairs

Modulating Hydrogen Shuttling in Ammonia by Neutral and Cationic Boron-Containing Frustrated Lewis Pairs (FLPs)

*Agamemnon E. Crumpton, Andreas Heilmann, and Simon Aldridge**

Abstract: Xanthene-backbone FLPs featuring secondary borane functions –B(Ar^X)H (where Ar^X = C_6F_5 (Ar^F) or C_6Cl_5 (Ar^{Cl})) have been targeted through reactions of the dihydroboranes $Me_2S{\cdot}BAr^XH_2$ with [4,5-xanth-(PR$_2$)Li]$_2$ (R = Ph, ^{i}Pr), and investigated in the synthesis of related cationic systems via hydride abstraction. The reactivity of these systems (both cationic and charge neutral) with ammonia have been probed, with a view to probing the potential for proton shuttling via N–H bond 'activation.' We find that in the case of four-coordinate boron systems (cationic or change neutral), the N–H linkage remains intact, supported by a NH···P hydrogen bond which is worth up to 17 kcal mol^{-1} thermodynamically, and enabled by planarization of the flexible xanthene scaffold. For cationic three coordinate systems, N-to-P proton transfer is viable, driven by the ability of the boron centre to stabilise the $[NH_2]^-$ conjugate base through N-to-B π bonding. This proton transfer can be shown to be reversible in the presence of excess ammonia, depending on the nature of the B-bound Ar^X group. It is viable in the case of C_6F_5 substituents, but is prevented by the more sterically encumbering and secondary donor-stabilising capabilities of the C_6Cl_5 substituent.

Introduction

In the realm of homogeneous catalysis and carbon-free fuel applications, the activation of ammonia (NH_3) has emerged as a valuable pursuit, driven by its high energy density and annual global production exceeding 176 million tonnes.[1,2] Despite the notable success of transition metal complexes in activating and transforming a wide range of E–H bonds, however, NH_3 activation poses a unique challenge due to its inclination to form stable Werner-ammine coordination complexes,[3] and the prohibitive gas-phase N–H bond dissociation energy of 99.4 kcal mol^{-1}.[4]

A significant area of recent research effort in small molecule activation has centred around alternative approaches based on main group element compounds.[5,6] Notably, Bertrand has employed cyclic (alkyl)-(amino)carbenes (CAACs) to effect NH_3 activation through insertion into the N–H bond, offering direct comparison with the limited number of *d*-block systems capable of oxidative addition.[7–15] More recent developments have explored alternative pathways, such as single-electron transfer from a dithiolene zwitterion or a Bi(II) complex,[16,17] as well as the thermoneutral and reversible splitting of NH_3 by Goicoechea and colleagues using a geometrically constrained phosphine.[18] Another ground-breaking contribution has come from Breher and co-workers, who demonstrated catalytic NH_3 transfer through a 'masked' frustrated Lewis pair (FLP) comprised of a phosphorus ylid and an aluminium Lewis acid.[19]

We have been interested in the chemistry of FLPs based on a xanthene backbone, and featuring phosphine Lewis base and borane Lewis acid components in the 4- and 5-positions (Figure 1).[20–22] In the case of systems such as xanth(PMes$_2$)(BAr$^F_2$), featuring both triaryl-borane and -phosphine functionalities, simple adduct formation is observed with ammonia via N→B bond formation. FLP systems featuring secondary borane units, –B(Ar)H, have been implicated in novel patterns of chemical reactivity,[23] and we were interested in targeting xanthene compounds of the type xanth(PR$_2$){B(Ar^X)H} (R = Ph, ^{i}Pr; Ar^X = Ar^F, C_6F_5 or Ar^{Cl}, C_6Cl_5).[24–29] We hypothesized that the H-substituent, while sterically less encumbering, would offer a chemical handle through which to modulate reactivity, for example via hydride abstraction to generate related boron-centred cations. In particular, we wanted to probe this approach to modulate N-to-P hydrogen shuttling via N–H bond 'activa-

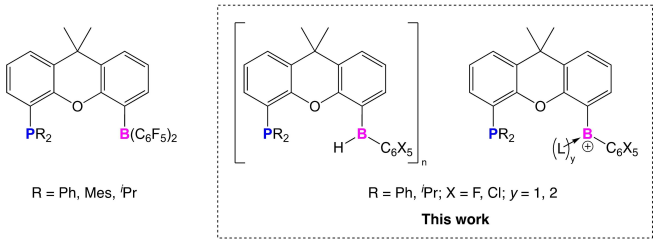

Figure 1. 4,5-Disubstituted xanthene derived FLPs relevant to the current study.

[*] A. E. Crumpton, Dr. A. Heilmann, Prof. S. Aldridge
Inorganic Chemistry Laboratory, Department of Chemistry, University of Oxford, South Parks Road, Oxford, OX1 3QR (UK)
E-mail: simon.aldridge@chem.ox.ac.uk

© 2024 The Authors. Angewandte Chemie published by Wiley-VCH GmbH. This is an open access article under the terms of the Creative Commons Attribution License, which permits use, distribution and reproduction in any medium, provided the original work is properly cited.

© 2024 The Authors. Angewandte Chemie published by Wiley-VCH GmbH

tion'. These studies, and the influence of the boron-bound aryl substituent thereon, are reported in this manuscript.

Results and Discussion

(i) Syntheses of Xanthene-Supported Secondary Borane/Phosphines

The reactions of the lithio-xanthene phosphines [4,5-xanth-$(PR_2)Li]_n$ (R = Ph, $n = 2$; R = ^{i}Pr, $n = 4$) with perhaloaryl-substituted boranes $Me_2S{\cdot}B(C_6X_5)H_2$ (X = F, Cl) in toluene (Scheme 1) lead to essentially quantitative conversion in each case to the anionic borates **1a–d** (in ca. 55–75 % isolated yields after recrystallization from hexanes). These complexes exhibit diagnostic triplet ^{11}B resonances (at δ_B = −20.3, −26.7, −19.6, and −26.1 ppm for **1a–d** respectively; $^1J_{BH} \approx 75$ Hz), typical of tetracoordinate boron hydrides, with the signals for the Ar^{Cl} derivatives (**1a/c**) shifted downfield of the Ar^F variants (**1b/d**).[24,30] Consistently, the ^{19}F NMR spectra of C_6F_5-containing compounds **1b/d** show splittings between the *meta* and *para* C–F resonances indicative of a tetrahedral geometry at boron ($\Delta\delta_{m,p}$ = 2.75, 3.12 ppm for **1b/d**, respectively).[31] Single-crystal X-ray diffraction studies confirm the connectivity implied by the spectroscopic data, and reveal coordination of the Li^+ cation by multiple donor sites (P, O, C, H, Cl/F), both intra- and intermolecular, leading to an overall oligomeric structure in each case (Figures 2 and S98–100).

The encapsulation of the Li cation within these phosphine/dihydroborate aggregates appears to have chemical (in addition to structural) implications, offering a potential explanation for the lack of reactivity of **1a–d** towards mild hydride abstraction reagents such as Me_3SiCl.[32] When each of **1a–d** is exposed to NH_3 (at 1 bar and 20 °C), however, crystalline solids are formed (**2a–d**: Scheme 2) which can be shown by single crystal X-ray diffraction in the cases of **2a**, **2b** and **2d**, to feature anion/cation pairs, $[Li(NH_3)_n]^+[xanth(PR_2)\{B(C_6X_5)H_2\}]^-$ (**a**, $n = 2$; **b**, $n = 3$; **d**, $n = 4$), which become increasingly separated as the number of bound ammonia ligands (n) increases. The Li^+ ion is coordinated by NH_3 ligands (n = 2–4) depending on the nature of the B-bound aryl group (Figure 2), in a manner familiar from ammoniate chemistry.[33,34] Removal of the NH_3 atmosphere leads to NH_3 uptake being rapidly reversed, with visible bubbling from the crystalline material and re-dissolution being complete within 5 min to regenerate **1a–d** (Scheme 2).

The cleavage of **1a–d** in the presence of amine donors and the possibility to access the target systems xanth(PR_2)-$\{B(C_6X_5)H\}$ (R = Ph, ^{i}Pr; X = F, Cl) by protic removal of the

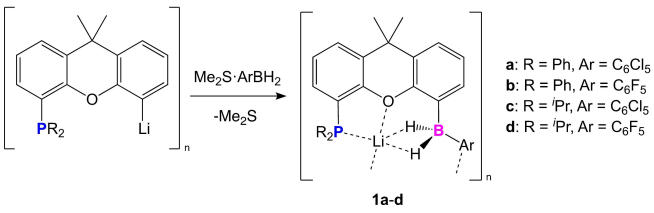

Scheme 1. Syntheses of lithium dihydroborates **1a–d** via the reactions of $[4,5\text{-Xanth}(PR_2)Li]_n$ (R = Ph, $n = 2$; R = ^{i}Pr, $n = 4$) with $Me_2S{\cdot}B(C_6X_5)H_2$ (X = F, Cl).

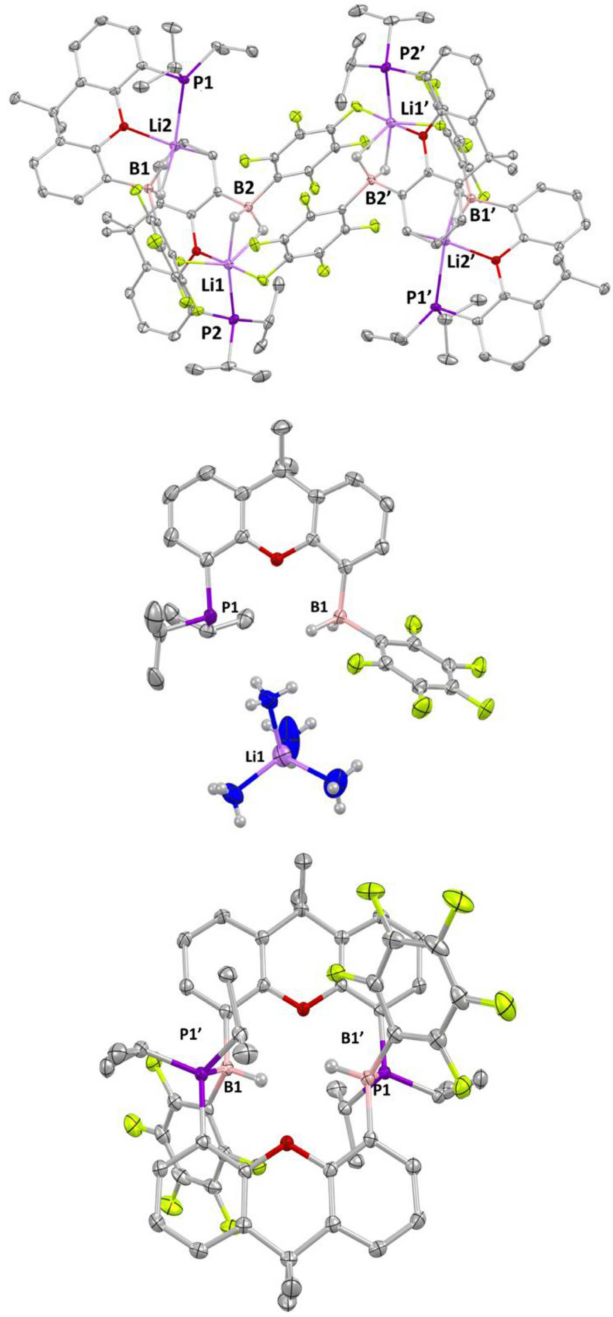

Figure 2. Molecular structures of (upper) **1d**, (centre) **2d** and (lower) **3d** in the solid state as determined by X-ray crystallography. Most H atoms omitted for clarity; thermal ellipsoids drawn at the 50% probability level (**1d**, **3d**) or the 30% level (**2d**). Key bond lengths (Å) and angles (°): (**1d**) P(2)–Li(2) 2.575(3), P(1)–Li(1) 2.519(3), O(1)–Li-(1) 2.029(3), O(2)–Li(2) 2.044(3), B(2)–Li(2) 2.274(4), B(1)–Li(1) 2.282(4); (**2d**) P(1)···Li(1) 5.197(4), O(1)···Li(1) 6.472(4), 5.197 B(1)···Li-(1) 4.969; (**3d**) P(1)–B(1′) 1.9895(18), C(14)–P(1)–B(1′)–C(2′) 178.44(9).

© 2024 The Authors. Angewandte Chemie published by Wiley-VCH GmbH

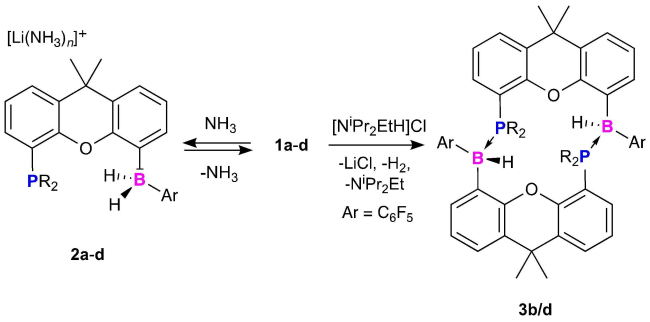

Scheme 2. De-aggregation of lithium dihydroborates **1a–d** via ammonia uptake/coordination at Li^+; use of the weak, sterically encumbered acid $[N^iPr_2EtH]^+$ to effect LiH removal and form the (dimeric) secondary borane/ phosphine complexes **3b/d** (for Ar = C_6F_5).

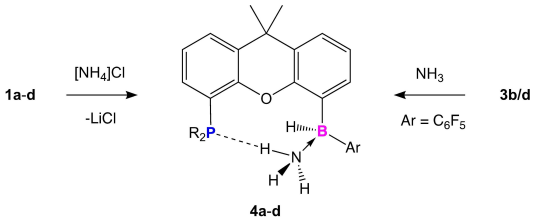

Scheme 3. Formation of ammonia adducts **4a–d** via protonolysis or substitution chemistry.

additional boron-bound hydride, led us to examine the reactivity of **1a–d** towards $[N^iPr_2EtH]Cl$. At room temperature these reactions lead to immediate effervescence, and in the cases of Ar^F-substituted systems **1b** and **1d**, the phosphine/borane products **3b/d** crystallize from a benzene solution. X-ray crystallography reveals that these two products are "head-to-tail" dimers of the P/B FLPs, with the phosphine donor of one molecule being bound to the borane function of the other, and vice versa (Figure 2). These systems are resolutely insoluble in compatible solvents, and cannot therefore be characterized in solution; both react with water (or water-containing solvents) via proto-deboronation, leading to loss of the borane function in the 5-position.

C_6Cl_5-containing systems **1a/c** also react with $[N^iPr_2EtH]Cl$ but in these cases an intractable mixture of P-/B-containing products results. We hypothesize that this is due to the additional steric and electronic demands of the C_6Cl_5 group (see below), which prevent dimerization, meaning that the putative (monomeric) FLPs xanth(PR_2){$B(C_6Cl_5)H$} (R = Ph, ^{i}Pr) remain in solution and are subject to further chemical attack (e.g. by $[N^iPr_2EtH]Cl$).[24]

(ii) Ammonia Adducts

Due to the insolubility of **3b/d** and the difficulty in accessing **3a/c** cleanly, we looked to pre-install the NH_3 molecule within the FLP frameworks directly via the reactions of **1a–d** with the parent ammonium cation $[NH_4]^+$ (as the Cl^- salt). This approach leads to the quantitative conversion of xanth(PR_2){$B(C_6X_5)H\cdot NH_3$} (R = Ph, ^{i}Pr; X = F, Cl), **4a–d** (Scheme 3). These ammonia adducts are each characterized by a broad single resonance in the ^{11}B NMR spectrum (at $\delta_B = -9.1$, -12.5, -10.5 and -13.5 ppm respectively), which taken together with a small magnitude of $\Delta\delta_{m,p}$ in the ^{19}F spectra of **4b/d** (4.85 and 4.89 ppm), are strongly indicative of a 4-coordinate boron centre bearing a single hydride. The N–H resonances in the respective ^1H NMR spectra are significantly shifted downfield ($\delta_H = 3.64$, 3.42, 3.86 and 3.56 ppm) relative to free NH_3 ($\delta_H = -0.14$ in C_6D_6).[35]

Previous work has shown that amine adducts of $B(C_6F_5)_3$ give rise to NH resonances that are downfield shifted, and the extent of this shift is influenced by secondary hydrogen-bond interactions and the nature of the associated H-bond acceptor.[36,37] Comparison with the chemical shift of $B(C_6F_5)_3\cdot NH_3$ itself (2.67 ppm in benzene-d_6) implies that the **4a–d** feature additional NH···X interactions, and X-ray crystallography reveals close contacts (2.6033(6), 2.6613(6) and 2.5974(6) Å for **4a–c**) featuring near-linear NH···P units (176.93(8), 169.67(11) and 173.34(15)°; Figure 3).[38–41] Previously detected gas phase NH···P interactions, are characterized by much longer (calculated) bond lengths.[38,41–43]

Structurally characterised examples of NH···P hydrogen bonds are surprisingly scarce, with few displaying the favourable close-to-linear alignment of the three atoms seen in **4a–c**.[38,41,44–47] The xanthene backbone in all three cases displays a near planar geometry (xanthene fold angles of **4a**:

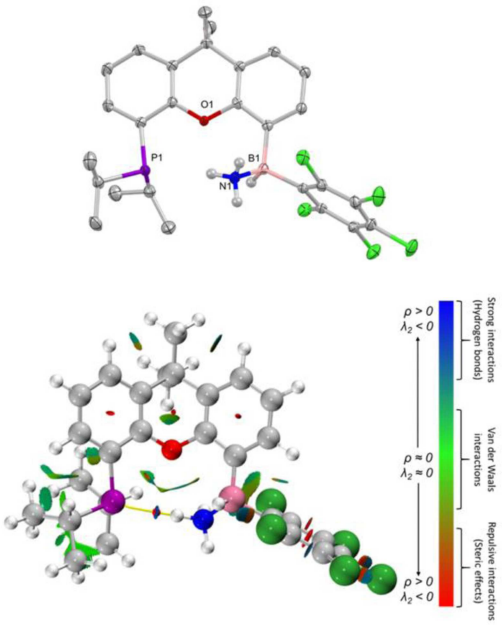

Figure 3. (upper) Molecular structure of **4c** in the solid state as determined by X-ray crystallography. Most H atoms omitted for clarity; thermal ellipsoids drawn at the 50% probability level. Key bond lengths (Å) and angles (°): B(1)–N(1) 1.611(4), N(1)H···P(1) 2.5974(6), N(1)–H···P(1) 173.34(15), xanthene fold angle 0.45(10); (lower) NCI plots of **4c**. The range of $\lambda_2\times\rho(r)$ used is -0.03 to $+0.02$ a.u. at $\sigma = 0.3$ a.u., QTAIM bond path in yellow with critical point in red.

© 2024 The Authors. Angewandte Chemie published by Wiley-VCH GmbH

5.67(6) °; **4b**: 4.97(7) °; **4c**: 0.45(10) °), rather than being puckered, thereby increasing the distance between the P and B substituents, and allowing for accommodation of the close-to-linear NH···P unit. Density functional theory (DFT) calculations (using the R^{2}SCAN-3c method) allow visualisation of hydrogen bonding through Non Covalent Interaction (NCI) plots,[48] and for **4a–c** these reveal unequivocal H-bonding regions between the P and N–H fragments (see Figure 3 for **4c**). Examination by the QT-AIM method reveals a bond critical point (BCP) in each case, lying between the P and N–H units, with a density of ca. 0.02 a.u. and a potential energy (ca. −0.011 a.u.), consistent with other reported calculations of hydrogen bonds.[49–51] Second-order perturbation theory using the Natural Bonding Orbitals (NBO) basis defines a hydrogen bond strength of 15.1/14.2 kcal mol^{-1} for the ^{i}Pr$_2$P-containing systems (**4c/d**), with the Ph$_2$P variants being weaker 4.6/3.1 kcal mol^{-1} (**4a/b**),[52] as expected based on the relative pK_as of the phosphines. Nonetheless, the hydrogen bonds in **4a–d** surpass previously calculated interactions for N–H···P systems.[53]

(iii) Reactivity of NH$_3$ in an FLP Context: Proton Shuttling

To increase the Lewis acidity of the boron centre in **4a–d** (and by extension the Brønsted acidity of the coordinated ammonia molecule), hydride abstraction from boron was effected using [Ph$_3$C][Al(OC(CF$_3$)$_3$)$_4$] (Scheme 4).[54] The resulting cations each give rise to an ^{11}B resonance at ca. 40 ppm (41.2, 39.3, 41.7 and 39.7 for **5a–d**, respectively), indicative of 3-coordinate boron. Transfer of an N–H proton to phosphorus is evident in the ^{31}P NMR spectrum, with the resonance shifted downfield of **4a–d** (and displaying a doublet coupling pattern) consistent with the formation of a P–H unit ($\delta_P = -3.0$, −2.7, 20.3 and 25.5 ppm for **5a–d**, respectively). In addition, the NH protons give rise to two distinct signals in a 1:1 ratio, implying hindered rotation around the B–N bond. Single-crystals suitable for diffraction could not be obtained for **5a–d**, but the use of the alternative [B(C$_6$F$_5$)$_4$]$^-$ counter-ion allowed the related salt **5a′** to be studied crystallographically. The structure of **5a′** confirms that the boron centre is indeed planar (sum of angles = 359.99°; Figure 4), with B = N double bond character implied by the short B–N distance of 1.383(3) Å.[55]

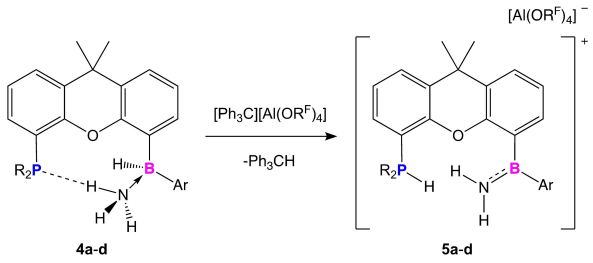

Scheme 4. N-to-P proton migration in **4a–d**, triggered by hydride abstraction at boron.

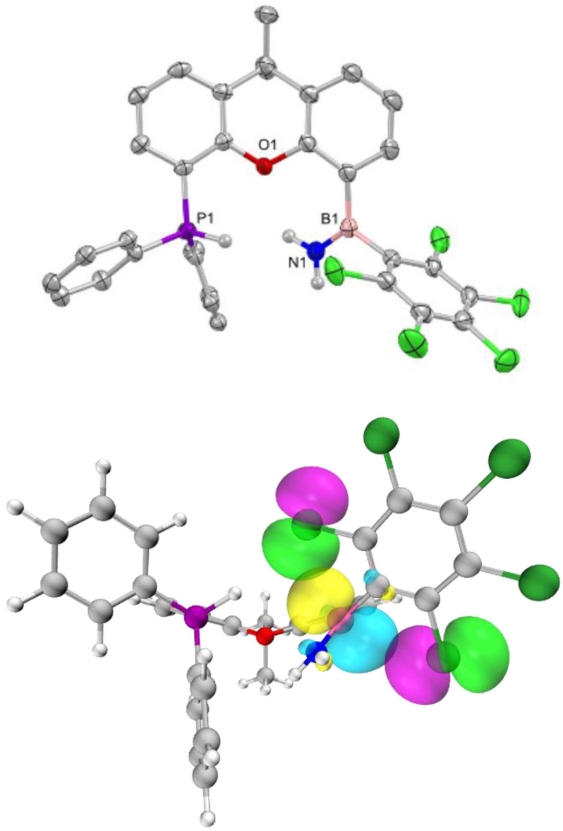

Figure 4. (upper) Molecular structure of **5a′** in the solid state as determined by X-ray crystallography. Most H atoms omitted for clarity; thermal ellipsoids drawn at the 50% probability level. Key bond lengths (Å) and angles (°): B(1)–N(1) 1.383(3), Cl(1 A)–B(1) 3.095(3), Cl(5 A)–B(1) 2.990(2), Cl(1B)–B(1) 3.110(15), Cl(5B)–B(1) 3.031(15), N(1)–B(1)–C(14)–C(28) plane to Ar^{Cl} 91.2(3), 83.9(15), xanthene fold angle 30.95(7) (lower) Natural orbitals from the second order perturbation theory analysis with isosurface values of 0.05 a.u. The Cl donor *p* orbitals are shown in magenta/green and the accepting vacant *p* orbital on boron in yellow/cyan.

Another structural feature apparent for **5a** in the solid state is the alignment of the Ar^{Cl} group orthogonal to the N–B–C–C plane (91.2(3), 83.9(15)°). While steric constraints are certainly important orientationally, the use of second-order perturbation theory also allows a donor/acceptor interaction to be identified between the two *ortho* chlorines and the boron centre, with a cumulative magnitude of 14.8 (for **5a**) or 14.5 kcal mol^{-1} (for **5c**); the equivalent F-to-B interactions in **5b/d** are much weaker (< 2 kcal mol^{-1}).[56] The effect of donation from the *ortho* chlorines is further seen in the calculated B–N Wiberg bond indices (WBIs), with **5a/c** possessing lower double bond character (1.196, 1.188) than **5b/d** (1.223, 1.234). While individual Cl→B interactions are weak, the WBI of 0.056 that they cumulatively contribute, signals an additional feature relevant to Ar^{Cl} groups that helps to explain their reactivity (see below).[57]

The accumulated data therefore suggest that the splitting of the coordinated ammonia molecule in **4a–d** on hydride abstraction (i.e. N–H to P–H conversion) reflects increased

© 2024 The Authors. Angewandte Chemie published by Wiley-VCH GmbH

acidity within the NH_3 moiety on conversion of a four-coordinate borane adduct to a three coordinate borenium cation, $-BAr^{F/Cl}(NH_3)^+$, and the potential for stabilization of the conjugate amide base (NH_2^-) through π-bond formation with the three-coordinate boron centre in **5a–d** (augmented by Cl→B donation in the case of the Ar^{Cl} derivatives).

With a view to exploring the reversibility of N-to-P proton transfer, the reactivity of **5a–d** to additional ammonia was probed. Exposure to NH_3 (at 1 bar pressure) leads to an immediate colour change from yellow to colourless (for the C_6F_5 systems) or pale yellow (for $Ar = C_6Cl_5$). Two different reaction pathways are revealed, depending on the nature of the boron-bound aryl groups (Scheme 5 and Figure 5). In the cases of the C_6Cl_5 systems **5a/c**, the reaction products (**7a/c**) give rise to ^{11}B resonances at ($\delta_B = 39.0/38.9$ ppm, respectively) indicative of three-coordinate boron. The doublet resonance in the ^{31}P spectrum of both **5a** and

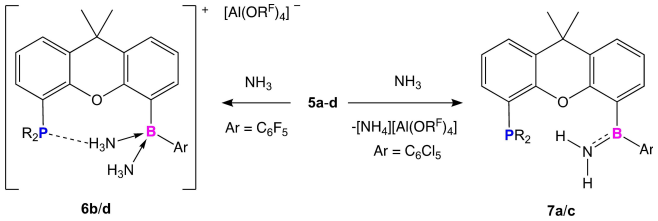

Scheme 5. Divergent reactivity of C_6F_5/C_6Cl_5-substituted systems **5b/d** and **5a/c** towards additional ammonia leading to the formation of boronium (**6b/d**) and borane products (**7a/c**).

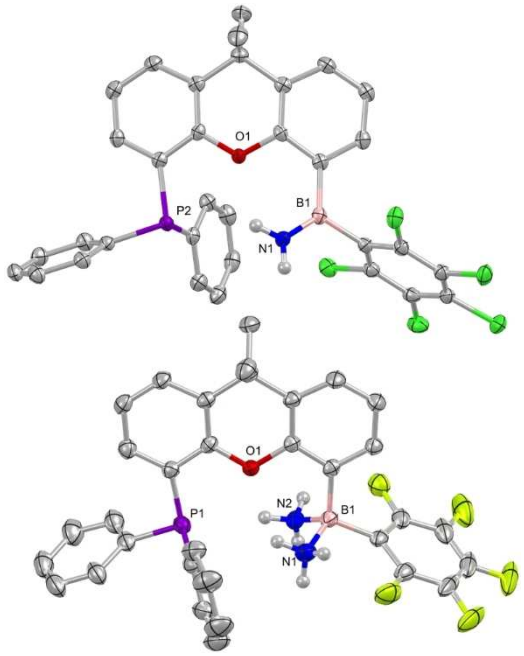

Figure 5. Molecular structures of (upper) **7a** and (lower) **6b** in the solid state as determined by X-ray crystallography. Most H atoms omitted for clarity and thermal ellipsoids drawn at the 50% probability level. Key bond lengths (Å) and angles (°): (**7a**) N(1)–B(1) 1.375(2), xanthene fold 15.55(5); (**6b**) N(3)H···P(2) 2.6897(10), N(2)H···P(1) 2.54(5), N(3)–H···P(2) 162.4(3), N(3)–H···P(2) 169(4).

5c collapses to a singlet and is shifted downfield (to $\delta_P = -18.7/-11.1$ ppm for **7a/c**). The solid-state structure of **7a** could be determined by X-ray crystallography, showing a structure very similar to the cationic component of **5a**, but with deprotonation of the P–H unit having occurred (sum of angles at phosphorus: **7a**: 304.4°; **5a**: 332.8°; Figure 5). Crystallization of the co-product $[NH_4][Al(OR^F)_4]$ was also possible, consistent with the hypothesis the added NH_3 had effected deprotonation of the phosphonium function.

By contrast, in the cases of the C_6F_5 systems **5b/d**, the products (**6b/d**) are characterized by ^{11}B resonances at ($\delta_B = -3.9$ and 3.2 ppm, respectively, with $\Delta\delta_{m,p}(^{19}F)$ values of 7.75/7.70 ppm, consistent a tetrahedral boron centre. As with **7a/c** the doublet resonance in the ^{31}P NMR spectrum collapses into a singlet and is shifted downfield (to $\delta_P = -18.9/-12.5$ ppm for **6b/d**, respectively). Additionally, the presence of coordinated NH_3 in **6b/d** is signalled by a very broad 6H ^1H NMR resonance at $\delta_H = 1.44/1.98$ ppm. A single-crystal diffraction study carried out on **6b** confirms the formation of a boronium cation, featuring two boron-bound NH_3 ligands, balanced by a $[Al(OR^F)_4]^-$ counter-anion (the asymmetric unit features two complete anion/cation pairs). The structure also features a N–H···P hydrogen bond analogous to those found in compounds of type **4** with short H···P contacts of 2.6897(10)/2.54(5) Å and N–H···P angles of 162.4(3)/169.0(40). Use of Second Order Perturbation Theory allows energies of 16.2/16.8 kcal mol^{-1} to be estimated for these interactions (for **6b/d**, respectively). With a broader perspective, the formation of **6b/d** in this manner provides evidence for reversal of N–H activation in the presence of excess NH_3.

DFT calculations were carried out to illuminate the different reaction pathways from **4a–d** (plus ammonia) in the presence of different B-bound aryl groups. Energetic barriers for the intramolecular activation of NH_3 following hydride abstraction are calculated to be very small (ca. 1 kcal mol^{-1} for the conversion of **4a–d** to **5a–d**, Figure 6). In similar fashion, the reverse reaction (H^+ transfer from P to NH_2) is also found to be very facile upon coordinating a second NH_3 molecule at boron (3.7, 3.5 kcal mol^{-1} for **5b/d** to **6b/d**, Figure 7). Pre-organization of the NH_3···P unit, through hydrogen bonding, aligns the phosphine lone pair and the N–H σ* orbital. When the Lewis acidity of the system is changed, by the removal of a hydride (to form a cationic boron centre), shuttling of a proton is extremely facile, as orbital alignment has already been achieved and the N–H bond has been weakened. Shutting of protons in this manner could be likened to the N–H–N hydrogen bond motifs in enzymatic reactions.[58,59]

The formation of different products from systems of type **5** (viz., **6b/d** or **7a/c**) depends crucially on the role of additional NH_3, i.e. whether it acts as a Brønsted base or a Lewis base coordinating at boron. Coordination of NH_3 is calculated to be a higher energy pathway (by 1–2 kcal mol^{-1}) for the C_6Cl_5 systems due to a combination of enhanced steric and Cl-to-B interactions above and below the borane plane (Figure 7). Conversely, the approach of NH_3 towards the phosphonium unit leading to deprotonation appears to be more facile. The activation barrier for attack at the

© 2024 The Authors. Angewandte Chemie published by Wiley-VCH GmbH

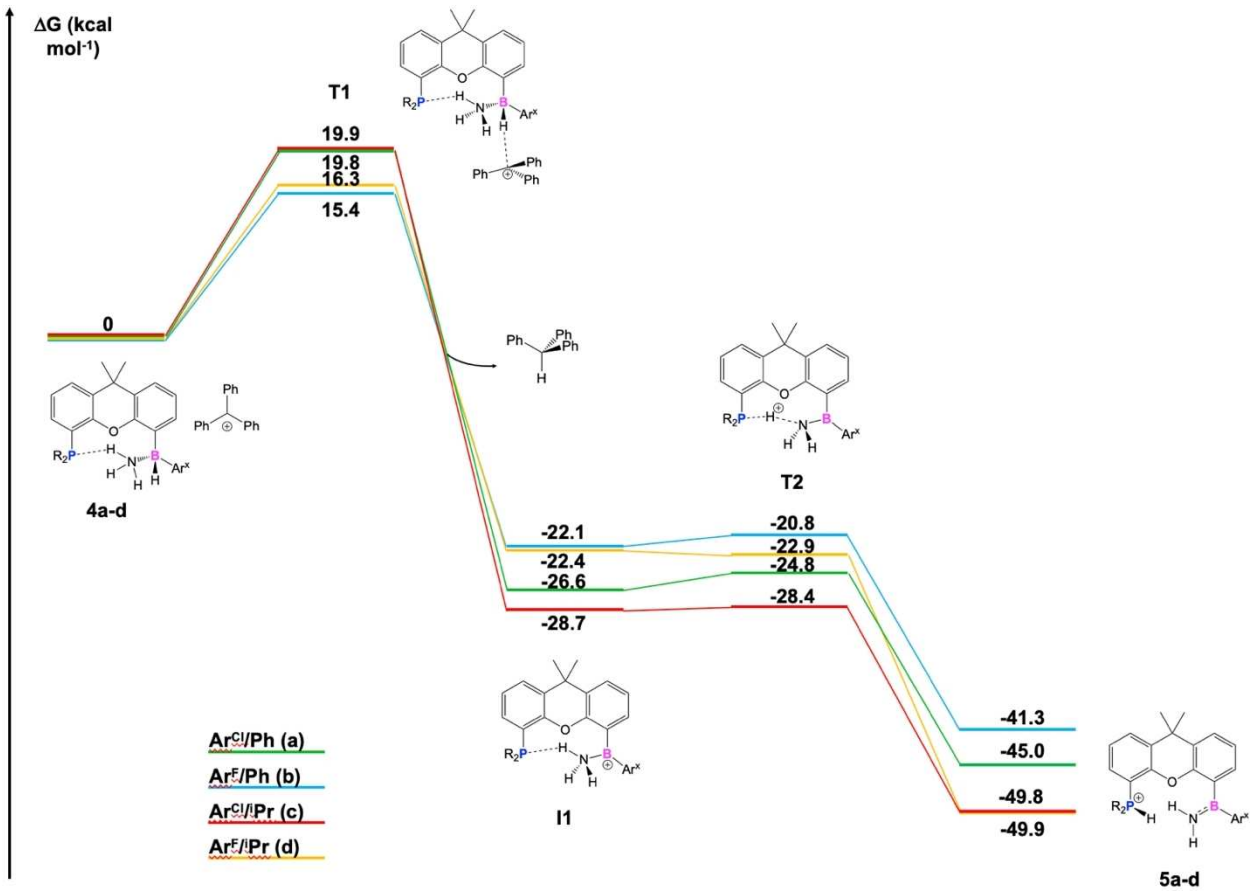

Figure 6. DFT calculated mechanism for the conversion of **4a–d** to **5a–d**; all free energies given in kcal mol^{-1} and referenced with respect to **4a–d**.

phosphonium unit is 15.7 kcal mol^{-1} for the P^{i}Pr$_2$ system (i.e. **5a** to **7a**) compared to 17.5 kcal mol^{-1} for coordination at the borane; for the PPh$_2$ analogue (**5c**) the barriers to approach to the P–H or borane units are very similar (19.3 mol^{-1} for **T3′** and 20.5 kcal mol^{-1} for **T3**). The morphology of the by-product is crucial to ensure the reaction is exergonic for **5c** to **7c**, with the $[NH_4]^+$ cation gaining considerable stability from the coordination of three NH_3 molecules (ca. 13 kcal mol^{-1}) and resulting in deprotonation being the lowest energy pathway (Supporting Information Table ST10). The boronium product is likely not favoured due too steric crowding of the tetracoordinate boron by the bulky Ar^{Cl} group.

For the Ar^{F} systems (**5b/d–6b/d**), the barriers for both processes were found to be much smaller (**5b–6b**, 12.7; **5b–7b**, 12.5; **5d–6d**, 15.2; **5d–7d** 17.3 kcal mol^{-1}, Figure 7) due to reduced steric effects and little donor stabilization at boron from the *ortho* fluorine atoms; the boronium products are also thermo-dynamically more favourable in both cases (**5b–6b**, −10.8; **5b–7b**, −2.0; **5d–6d**, −1.7; **5d–7d** 6.9 kcal mol^{-1}).

Conclusions

Xanthene-backbone FLPs featuring the 2° borane functions –B(Ar^{F})H and –B(Ar^{Cl})H can be synthesized in good yield through reactions of the dihydroboranes Ar^{X}BH$_2$ with [4,5-xanth(PR$_2$)Li]$_2$ (R = Ph, ^{i}Pr), and have been investigated as precursors for related cationic systems via hydride abstraction. The reactivity of these systems with ammonia has been examined, in order to probe the potential for proton shuttling via N–H bond cleavage. In the case of four-coordinate boron systems (both cationic and charge neutral), the N–H linkage remains intact, supported by strong, close-to-linear NH···P hydrogen bonds, enabled in turn by planarization of the flexible xanthene scaffold. For cationic three coordinate systems, N-to-P proton transfer is viable, driven by the ability of the borane to stabilise the $[NH_2]^-$ conjugate base through N-to-B π bonding. This proton transfer can be shown to be reversible in the presence of excess ammonia (depending on the nature of the B-bound Ar^{X} group), thereby showcasing a phenomenon which has not previously been observed in FLP systems. Reversibility is viable in the case of C_6F_5 substituents, but is prevented by the more sterically encumbering and secondary donor-stabilising capabilities of the C_6Cl_5 substituent.[60]

© 2024 The Authors. Angewandte Chemie published by Wiley-VCH GmbH

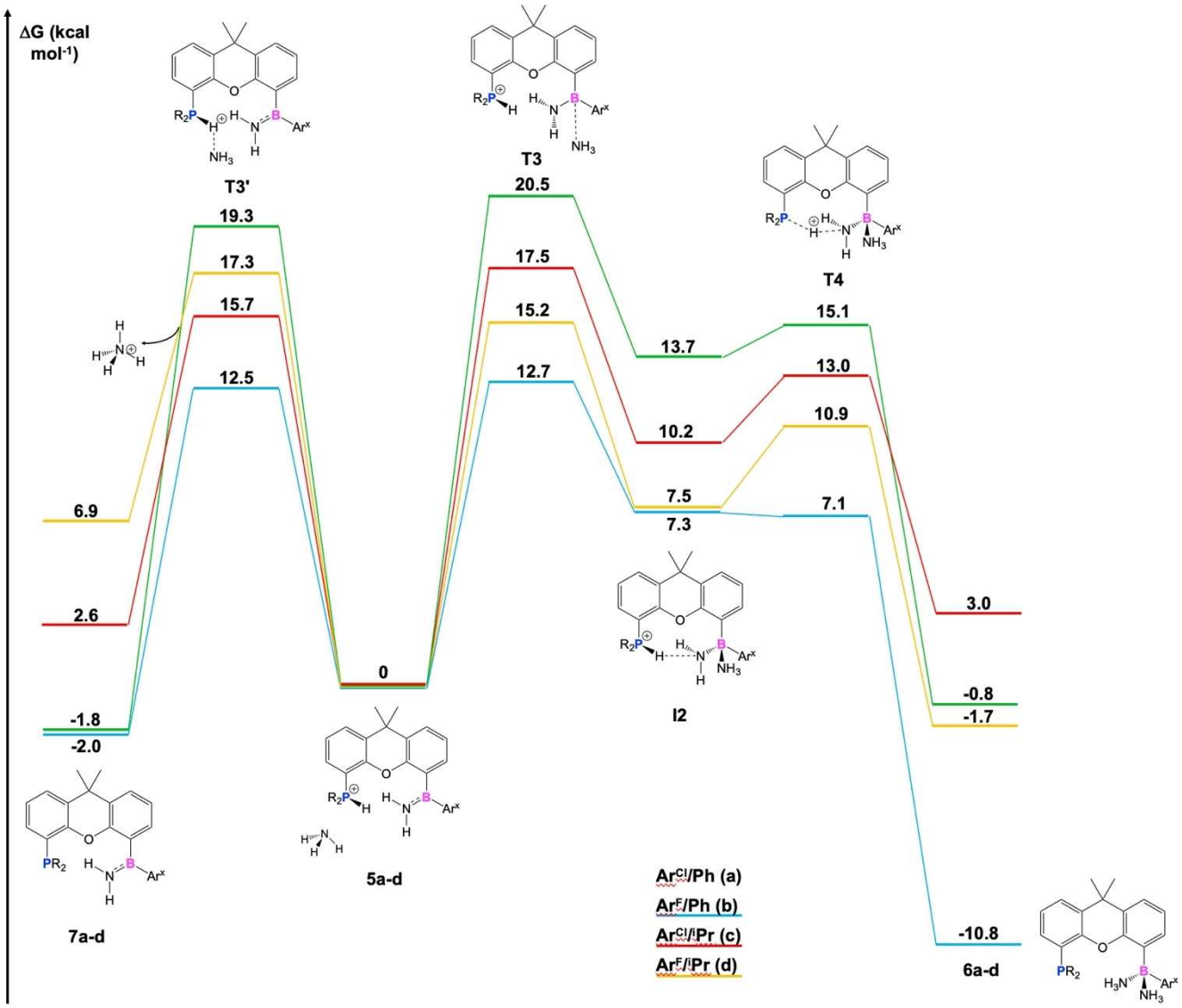

Figure 7. DFT calculated mechanism for the conversion of **5a–d** to either **6a–d** or **7a–d**; all free energies given in kcal mol^{-1} and referenced with respect to **5a–d**.

Supporting Information

The data that support the findings of this study are available in the supplementary material of this article. Included are full synthetic and characterizing data, representative spectra and details of the X-ray crystal structures and quantum chemical calculations. Details of the X-ray crystal structures described in this paper are available from the CCDC, deposition numbers 2343486–2343489, 2343491–2343499 and 2343501–2343504. The authors have cited additional references within the Supporting Information.[61–85]

Acknowledgements

We thank the EPSRC Centre for Doctoral Training in Inorganic Chemistry for Future Manufacturing (OxICFM; EP/S023828/1) and the Leverhulme Trust (RP-2018-246). We thank Dr Eugene Kolychev for determining the X-ray crystal structure of $[xanth(PPh_2)Li(thf)]_2$.

Conflict of Interest

The authors declare no conflict of interest.

Data Availability Statement

The data that support the findings of this study are available in the supplementary material of this article.

© 2024 The Authors. Angewandte Chemie published by Wiley-VCH GmbH

Keywords: Frustrated Lewis Pair · ammonia · borane · phosphine · quantum chemical calculations

[1] B. David, F. Armstrong, P. Bowen, D. Fowler, J. Irvine, L. Murciano, *Ammonia: Zero-Carbon Fertiliser, Fuel and Energy Store*, POLICY BRIEFING, London **2020**.
[2] J. I. Van der Vlugt, *Chem. Soc. Rev.* **2010**, *39*, 2302–2322.
[3] A. Werner, *Z. Anorg. Chem.* **1893**, *3*, 267–300.
[4] M. J. Bezdek, S. Guo, P. J. Chirik, *Science* **2016**, *354*, 730–733.
[5] M. M. Hansmann, G. Bertrand, *J. Am. Chem. Soc.* **2016**, *138*, 15885–15888.
[6] C. Weetman, S. Inoue, *ChemCatChem.* **2018**, *10*, 4213–4228.
[7] G. D. Frey, V. Lavallo, B. Donnadieu, W. W. Schoeller, G. Bertrand, *Science* **2007**, *316*, 439–441.
[8] J. Zhao, A. S. Goldman, J. F. Hartwig, *Science* **2005**, *307*, 1080–1082.
[9] T. Braun, *Angew. Chem. Int. Ed.* **2005**, *44*, 5012–5014.
[10] C. M. Fafard, D. Adhikari, B. M. Foxman, D. J. Mindiola, O. V. Ozerov, *J. Am. Chem. Soc.* **2007**, *129*, 10318–10319.
[11] E. Morgan, D. F. MacLean, R. McDonald, L. Turculet, *J. Am. Chem. Soc.* **2009**, *131*, 14234–14236.
[12] R. Koelliker, D. Milstein, *Angew. Chem. Int. Ed.* **1991**, *30*, 707–709.
[13] E. B. Hulley, J. B. Bonanno, P. T. Wolczanski, T. R. Cundari, E. B. Lobkovsky, *Inorg. Chem.* **2010**, *49*, 8524–8544.
[14] Y. Nakajima, H. Kameo, H. Suzuki, *Angew. Chem. Int. Ed.* **2006**, *45*, 950–952.
[15] M. A. Salomon, A. K. Jungton, T. Braun, *Dalton Trans.* **2009**, 7669–7677.
[16] Y. Wang, P. M. Tran, M. E. Lahm, Y. Xie, P. Wei, E. R. Adams, J. N. Glushka, Z. Ren, V. V. Popik, H. F. Schaefer, G. H. Robinson, *J. Am. Chem. Soc.* **2022**, *144*, 16325–16331.
[17] X. Yang, E. J. Reijerse, K. Bhattacharyya, M. Leutzsch, M. Kochius, N. Nöthling, J. Busch, A. Schnegg, A. A. Auer, J. Cornella, *J. Am. Chem. Soc.* **2022**, *144*, 16535–16544.
[18] J. Abbenseth, O. P. E. Townrow, J. M. Goicoechea, J. Abbenseth, O. P. E. Townrow, J. M. Goicoechea, *Angew. Chem.* **2021**, *133*, 23817–23821.
[19] F. Krämer, J. Paradies, I. Fernández, F. Breher, *Nat. Chem.* **2024**, *16*, 63–69.
[20] P. Vasko, I. A. Zulkifly, M. Á. Fuentes, Z. Mo, J. Hicks, P. C. J. Kamer, S. Aldridge, *Chem. Eur. J.* **2018**, *24*, 10531–10540.
[21] Z. Mo, A. Rit, J. Campos, E. L. Kolychev, S. Aldridge, *J. Am. Chem. Soc.* **2016**, *138*, 3306–3309.
[22] Z. Mo, E. L. Kolychev, A. Rit, J. Campos, H. Niu, S. Aldridge, *J. Am. Chem. Soc.* **2015**, *137*, 12227–12230.
[23] M. A. Légaré, M. A. Courtemanche, É. Rochette, F. G. Fontaine, *Science* **2015**, *349*, 513–516.
[24] A. E. Ashley, T. J. Herrington, G. G. Wildgoose, H. Zaher, A. L. Thompson, N. H. Rees, T. Kr, D. O'hare, *J. Am. Chem. Soc.* **2011**, *133*, 14727–14740.
[25] H. Zhao, J. H. Reibenspies, F. P. Gabbaï, *Dalton Trans.* **2012**, *42*, 608–610.
[26] H. Zaher, A. E. Ashley, M. Irwin, A. L. Thompson, H. Zaher, T. Krämer, D. O'Hare, *Chem. Commun.* **2013**, *49*, 9755–9757.
[27] E. J. Lawrence, R. J. Blagg, D. L. Hughes, A. E. Ashley, G. G. Wildgoose, *Chem. Eur. J.* **2015**, *21*, 900–906.
[28] R. J. Blagg, T. R. Simmons, G. R. Hatton, J. M. Courtney, E. L. Bennett, E. J. Lawrence, G. G. Wildgoose, *Dalton Trans.* **2016**, *45*, 6032–6043.
[29] R. J. Blagg, G. G. Wildgoose, *RSC Adv.* **2016**, *6*, 42421–42427.
[30] B. Singaram, T. E. Cole, H. C. Brow, *Organometallics* **1984**, *3*, 1520–1523.
[31] A. G. Massey, A. J. Park, *J. Organomet. Chem.* **1966**, *5*, 218–225.
[32] R. J. Blagg, T. R. Simmons, G. R. Hatton, J. M. Courtney, E. L. Bennett, E. J. Lawrence, G. G. Wildgoose, *Dalton Trans.* **2016**, *45*, 6032.
[33] R. Neufeld, R. Michel, R. Herbst-Irmer, R. Schöne, D. Stalke, *Chem. Eur. J.* **2016**, *22*, 12340.
[34] R. Michel, R. Herbst-Irmer, D. Stalke, *Organometallics* **2010**, *29*, 6169–6171.
[35] T. Shima, J. Yang, G. Luo, Y. Luo, Z. Hou, *J. Am. Chem. Soc.* **2020**, *142*, 9007–9016.
[36] A. J. Mountford, S. J. Lancaster, S. J. Coles, P. N. Horton, D. L. Hughes, M. B. Hursthouse, M. E. Light, *Inorg. Chem.* **2005**, *44*(16), 5921–5933.
[37] A.-M. Fuller, A. J. Mountford, S. J. Coles, P. N. Horton, D. L. Hughes, M. B. Hursthouse, L. Male, S. J. Lancaster, *Dalton Trans.* **2008**, 6381–6392.
[38] M. Hasegawa, H. Noda, *Nature* **1975**, *254*, 212–212.
[39] A. Shahi, E. Arunan, *J. Chem. Sci.* **2016**, *128*, 1571–1577.
[40] T. Steiner, *Angew. Chem. Int. Ed.* **2002**, *41*, 1433–7851.
[41] E. Arunan, G. R. Desiraju, R. A. Klein, J. Sadlej, S. Scheiner, I. Alkorta, D. C. Clary, R. H. Crabtree, J. J. Dannenberg, P. Hobza, H. G. Kjaergaard, A. C. Legon, B. Mennucci, D. J. Nesbitt, *Pure Appl. Chem.* **2011**, *83*, 1619–1636.
[42] K. H. Møller, A. S. Hansen, H. G. Kjaergaard, *J. Phys. Chem. A* **2015**, *119*, 10988–10998.
[43] A. S. Hansen, L. Du, H. G. Kjaergaard, *J. Phys. Chem. Lett.* **2014**, *5*, 4225–4231.
[44] Y. Matano, M. Nakashima, T. Nakabuchi, H. Imahori, S. Fujishige, H. Nakano, *Org. Lett.* **2008**, *10*, 553–556.
[45] J. Andrieu, C. Baldoli, S. Maiorana, R. Poli, P. Richard, *Eur. J. Org. Chem.* **1999**, 2909–2914.
[46] S. E. Durran, M. R. J. Elsegood, S. R. Hammond, M. B. Smith, *Dalton Trans.* **2010**, *39*, 7136–7146.
[47] S. Kammerer, B. Neumann, B. Köhler, P. Mayer, I. P. Lorenz, *Z. Anorg. Allg. Chem.* **2013**, *639*, 1173–1180.
[48] E. R. Johnson, S. Keinan, P. Mori-Sánchez, J. Contreras-García, A. J. Cohen, W. Yang, *J. Am. Chem. Soc.* **2010**, *132*, 6498–6506.
[49] R. F. W. Bader, *Acc. Chem. Res.* **1975**, *8*, 34–40.
[50] R. F. W. Bader, *Acc. Chem. Res.* **1985**, *18*, 9–15.
[51] S. Emamian, T. Lu, H. Kruse, H. Emamian, *J. Comput. Chem.* **2019**, *40*, 2868–2881.
[52] E. D. Glendening, C. R. Landis, F. Weinhold, *J. Comput. Chem.* **2019**, *40*, 2234–2241.
[53] P. Gilli, L. Pretto, V. Bertolasi, G. Gilli, *Acc. Chem. Res.* **2009**, *42*, 33–44.
[54] I. Krossing, H. Brands, R. Feuerhake, S. Koenig, *J. Fluorine Chem.* **2001**, *112*, 83–90.
[55] A. Maier, M. Hofmann, H. Pritzkow, W. Siebert, *Angew. Chem. Int. Ed.* **2002**, *41*.
[56] I. Ara, J. Forniés, M. A. García-Monforte, A. Martín, B. Menjón, *Chem. Eur. J.* **2004**, *10*, 4186–4197.
[57] T. Lu, F. Chen, *J. Phys. Chem. A* **2013**, *117*, 3100–3108.
[58] S. O. Shan, D. Herschlag, *Methods Enzymol.* **1999**, *308*, 246–276.
[59] S. Dajnowicz, J. M. Parks, X. Hu, K. Gesler, A. Y. Kovalevsky, T. C. Mueser, *J. Biol. Chem.* **2017**, *292*, 5970–5980.
[60] Details of the X-ray crystal structures described in this paper are available from the CCDC, deposition numbers 2343486–2343489, 2343491–2343499 and 2343501–2343504.
[61] F. Song, R. D. Cannon, S. J. Lancaster, M. Bochmann, *J. Mol. Catal. A* **2004**, *218*, 21–28.
[62] J. Cosier, A. M. Glazer, *J. Appl. Crystallogr.* **1986**, *19*, 105–107.
[63] CrysAlisPro v.1.171.42.70a, Agilent Technologies **2011**.
[64] G. M. Sheldrick, *Acta Crystallogr.* **2015**, *C71*, 3–8.
[65] G. M. Sheldrick, *Acta Crystallogr.* **2015**, *A71*, 3–8.
[66] O. V. Dolomanov, L. J. Bourhis, R. J. Gildea, J. A. K. Howard, H. Puschmann, *J. Appl. Crystallogr.* **2009**, *42*, 339–341.

© 2024 The Authors. Angewandte Chemie published by Wiley-VCH GmbH

[67] F. Neese, J. Wiley, *Wiley Interdiscip. Rev.: Comput. Mol. Sci.* **2012**, *2*, 73–78.
[68] F. Neese, *Wiley Interdiscip. Rev.: Comput. Mol. Sci.* **2018**, *8*, e1327.
[69] F. Neese, F. Wennmohs, U. Becker, C. Riplinger, *J. Chem. Phys.* **2020**, *152*, 224108.
[70] J. W. Furness, A. D. Kaplan, J. Ning, J. P. Perdew, J. Sun, *J. Phys. Chem. Lett.* **2020**, *11*, 8208–8215.
[71] S. Grimme, A. Hansen, S. Ehlert, J. M. Mewes, *J. Chem. Phys.* **2021**, *154*, 64103.
[72] E. Caldeweyher, S. Ehlert, A. Hansen, H. Neugebauer, S. Spicher, C. Bannwarth, S. Grimme, *J. Chem. Phys.* **2019**, *150*, 154122.
[73] H. Kruse, S. Grimme, *J. Chem. Phys.* **2012**, *136*, 154101.
[74] M. D. Hanwell, D. E. Curtis, D. C. Lonie, T. Vandermeersch, E. Zurek, G. R. Hutchison, *J. Cheminf.* **2012**, *4*, 1–17.
[75] J.-D. Chai, M. Head-Gordon, *J. Chem. Phys.* **2008**, *128*, 084106.
[76] J.-D. Chai, M. Head-Gordon, *Phys. Chem. Chem. Phys.* **2008**, *10*, 6615–6620.
[77] F. Weigend, R. Ahlrichs, *Phys. Chem. Chem. Phys.* **2005**, *7*, 3297–3305.
[78] F. Weigend, *Phys. Chem. Chem. Phys.* **2006**, *8*, 1057–1065.
[79] V. Barone, M. Cossi, *J. Phys. Chem. A* **1998**, *102*, 1995–2001.
[80] *NBO 7.0.*, E. D. Glendening, J, K. Badenhoop, A. E. Reed, J. E. Carpenter, J. A. Bohmann, C. M. Morales, P. Karafiloglou, C. R. Landis, F. Weinhold, Theoretical Chemistry Institute, University of Wisconsin, Madison **2018**.
[81] T. Lu, F. Chen, *J. Comput. Chem.* **2012**, *33*, 580–592.
[82] E. D. Glendening, C. R. Landis, F. Weinhold, *J. Comput. Chem.* **2019**, *40*, 2234–2241.
[83] F. Cortés-Guzmán, R. F. W. Bader, *Coord. Chem. Rev.* **2005**, *249*, 633–662.
[84] E. R. Johnson, S. Keinan, P. Mori-Sánchez, J. Contreras-García, A. R. Cohen, W. Yang, *J. Am. Chem. Soc.* **2010**, *132*, 6498–6506.
[85] J. Contreras-García, W. Yang, E. R. Johnson, *J. Phys. Chem. A* **2011**, *115*, 12983–12990.

Manuscript received: April 4, 2024
Accepted manuscript online: May 31, 2024
Version of record online: ■■, ■■

© 2024 The Authors. Angewandte Chemie published by Wiley-VCH GmbH

Forschungsartikel

Frustrated Lewis Pairs

A. E. Crumpton, A. Heilmann, S. Aldridge* — **e202406440**

Modulating Hydrogen Shuttling in Ammonia by Neutral and Cationic Boron-Containing Frustrated Lewis Pairs (FLPs)

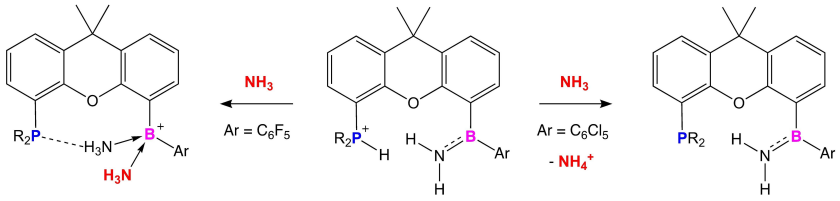

Xanthene-backbone FLPs featuring secondary borane functions –B(Ar)H (where Ar = C_6F_5 or C_6Cl_5) have been synthesized, and investigated for the generation of related cationic systems via hydride abstraction. The reactivity of these systems (both cationic and charge neutral) with ammonia have been probed, with a view to probing the potential for proton shuttling via N–H bond 'activation.'

© 2024 The Authors. Angewandte Chemie published by Wiley-VCH GmbH